Self-propagating combustion of sputter-deposited Al/CuO nanolaminates

James Zapata, Andréa Nicollet, Baptiste Julien, Guillaume Lahiner, Alain Estève, Carole Rossi

▶ **To cite this version:**

James Zapata, Andréa Nicollet, Baptiste Julien, Guillaume Lahiner, Alain Estève, et al.. Self-propagating combustion of sputter-deposited Al/CuO nanolaminates. Combustion and Flame, 2019, 205, pp.389-396. 10.1016/j.combustflame.2019.04.031 . hal-02127351

HAL Id: hal-02127351
https://hal.science/hal-02127351

Submitted on 13 May 2019

HAL is a multi-disciplinary open access archive for the deposit and dissemination of scientific research documents, whether they are published or not. The documents may come from teaching and research institutions in France or abroad, or from public or private research centers.

L'archive ouverte pluridisciplinaire **HAL**, est destinée au dépôt et à la diffusion de documents scientifiques de niveau recherche, publiés ou non, émanant des établissements d'enseignement et de recherche français ou étrangers, des laboratoires publics ou privés.

https://doi.org/10.1016/j.combustflame.2019.04.031

To cite it : Combustion and Flame, Volume 205, July 2019, Pages 389-396

Self-propagating combustion of sputter-deposited Al/CuO nanolaminates

James Zapata, Andrea Nicollet, Baptiste Julien, Guillaume Lahiner, Alain Esteve, Carole Rossi*

CNRS, LAAS, University of Toulouse, 7 avenue du Colonel Roche, F-31400 Toulouse, France

*Corresponding author: Carole Rossi; email : rossi@laas.fr

DRAFT

Abstract

The complex Al/CuO self-propagating reaction involving multi-phase and multi-species dynamics was studied in order to investigate the very high flame temperature around the vaporization temperature of alumina, even under a neutral environment. Experiments were performed on different sputter-deposited Al/CuO multilayers coupling optical spectroscopy with high speed camera measurements. The clear presence of both AlO and Al signatures in gas phase suggests that the redox reaction starts in the bulk nanolaminate, which then rapidly tear off the substrate to continue burning in a heterogeneous (condensed and gas) phase in the environment. The flame temperature increases with the stoichiometry but is independent of the bilayer thickness. In addition to the confirmation of the effects of stoichiometry and the bilayer thickness on the characteristics of the self-propagating reaction, the predominant role of

https://doi.org/10.1016/j.combustflame.2019.04.031

To cite it : Combustion and Flame, Volume 205, July 2019, Pages 389-396

process-induced residual stress was highlighted for the first time; it can lead to an early disruption of the multilayer long before the completion of the redox reaction.

Keywords: self-propagation reactions, energetic materials, CuO, Al, Al/CuO nanolaminates

1. Introduction

Thermite multilayered films, also referred to as nanolaminates, composed of alternating thin layers (tens to hundreds of nm thick) of metal/oxidizers, have various uses in microelectromechanical systems (MEMS)[1-4], microelectronics and materials bonding applications[5-7]. From a technological perspective, the emergence and development of thermite multilayers have benefited from the versatile magnetron sputtering technique, which enables the reliable deposition of high-quality, well-adhered metallic and oxide materials at commercially competitive rates. In particular, DC magnetron-sputtering has developed rapidly over the last decade to become a standard manufacturing process for Al/CuO nanothermites; its relatively low cost and easy application to the fabrication of large-area films make it possible to envision the transfer into industrial products. This specific Al/CuO system is widely used for in micro initiation or exploding foil initiators[8-11] because of its high volumetric energy density (> 13 kJ/cm^3) and its propensity to produce hot gas.

From a material point of view, after almost two decades of research in sputter-deposited multilayered thermites, it has been proven that Al/CuO multilayers can have a very low ignition temperature (below the Al melting point) and enhanced reactivity with optimization or manipulation of the bilayer thickness, the stoichiometric ratio or the number of bilayers [11]. The redox reaction kinetics have been widely studied under a slow heating rate (10 K.min^{-1}) using calorimetric analysis such as differential scanning calorimetry or thermogravimetric

https://doi.org/10.1016/j.combustflame.2019.04.031
To cite it : Combustion and Flame, Volume 205, July 2019, Pages 389-396

analysis [12-15]. A recent work from Abdallah *et al*. showed that exothermic chemical reactions are controlled by the outward migration of oxygen atoms from the CuO matrix (at temperature as low as 350 °C) towards the aluminum layers through the final oxide layer. They also clearly established that the chemical reaction rate strongly depends on the final oxide nature (Al_2O_3) affecting the oxygen diffusivity [16, 17]. With the goal of approaching the combustion event, other studies combine high heating rates (up to roughly 10^5 $K.s^{-1}$) with mass spectroscopy or dynamic imaging microscopy at even higher heating rates (~10^{11} $K.s^{-1}$). A recent study by Egan *et al* used high heating rate analytics [14] to determine the effect of bilayer thickness on reaction mechanisms in Al/CuO nanolaminates. They observed the rapid loss of the nanostructure occurring about two orders of magnitude faster than the gas – condensed heterogeneous reaction, confirming the dominance of the condensed phase reaction at the nanoscale. In another work, DeLisio *et al.* studied the effect of stoichiometry and bilayer thickness [12, 18] on the ignition and reaction dynamics of Al/CuO nanolaminates [19].

As the majority of applications of Al/CuO nanolaminates as micro initiations are contingent upon the control of energy/power release, a quantification of the flame temperature coupled with an analysis of the gaseous products during the self-propagating reaction under atmospheric conditions is necessary for the development of smart energetic layers that can be accurately tuned to maximize the energy and power outputs [20]. Only a few studies have investigated self-propagating themite reactions. Kinsey *et al.* in [5] showed that enriching the Al/Cu_2O nanothermite with Cu permits significant reduction of the self-propagating reaction velocity and temperature, highlighting the impact of material properties on the energy release pathways. Another recent work [21], studying the flame propagation of Al/CuO nanothermites in confined configurations observed two different combustion-stages : a fast ignition followed by a slow combustion without an in-depth understanding of the reaction pathways. In [11], Nicollet *et al*.

https://doi.org/10.1016/j.combustflame.2019.04.031
To cite it : Combustion and Flame, Volume 205, July 2019, Pages 389-396

captured the flame signature during Al/CuO reaction in nanolaminates with various dimensional features using a photodiode (VISHAY reference BPV10, 380-1100 nm range). They often observed two regimes (see Supplementary File Figure S1) without further explanation. Just after the ignition, the flame is characterized by a very intense peak followed by a slower and less intense combustion regime.

Despite these experimental findings, there is still much that is unknown about the physics and processes controlling the self-propagating reaction front in reactive nanolaminates, in terms of temperature and gas release. This work proposes to combine fast optical spectroscopy with high speed camera measurement in order to examine the very high flame temperature (well above the adiabatic flame temperature of 2967 K) reported in the litterature (3800 K [22] and 3000-6000 K [23]) and to suggest a possible self-propagating combustion scenario in Al/CuO multilayers. Importantly, we not only confirm the effect of stoichiometric ratio and bilayer thickness on self-propagating reaction characteristics, but, for the first time, we discuss and highlight the stress-induced disintegration of the multilayer prior to the completion of the reaction of Al within the layers, which impacts the reaction properties in terms of propagation front velocity and flame temperature.

2. Experimental

2.1. Combustion front characterization setup

The self-propagating reaction velocity is characterized with a SA3 Photron high-speed camera with a maximum of 120,000 fps. A 6 cm long by 1.6 mm wide line of Al/CuO multilayers is deposited onto a Kapton low conductive substrate. Three titanium filaments (100 µm width) are patterned underneath the nanothermite line. One is positioned at one end of the line to resistively heat the multilayer to its ignition point. The other two filaments are positioned at the

https://doi.org/10.1016/j.combustflame.2019.04.031
To cite it : Combustion and Flame, Volume 205, July 2019, Pages 389-396

other end of the line and separated by 0.8 cm to capture the combustion front path: a current of 40 mA is supplied to these two filaments and the voltage through a dummy 1 kΩ resistance is recorded on an oscilloscope to detect the passage of the combustion front. The propagation of the combustion front is thus monitored using both the high-speed camera and the measurement of the travel time between the two titanium filaments. In parallel, the optical emission spectrum produced by the combustion event is captured by an optical fiber and sent to a spectrometer (AvaSpecULS2048CL-EVO spectrometer, Avantes Inc.). A 6 mm diameter collimating lens (confocal length 8.7 mm) is placed at approximately 40 mm from the propagating front to capture light. The spectrometer has a quoted resolution, for the given slit and grating, of 0.06-20 nm. The system is calibrated using a HG-1 mercury-argon calibration source from Ocean Optics, Inc.

Figure 1 shows the experimental setup scheme employed in the self-propagating combustion experiments.

2.2. Al/CuO sputter-deposited nanolaminates

The multilayer stacks were chosen to be consistent with previous work [17, 20]. They consist of 10 sputter-deposited bilayers (see Figure 2). To study the influence of the bilayer thickness and stoichiometry on the self-propagating combustion velocity, several samples of varying bilayer thicknesses (*w)* were deposited using two different sputter-depositing systems and conditions :

- UNIVEX multi-purpose experimentation systems, developed by Leybold company (Swedish group ATLAS Copco): one set of samples were magnetron sputtered from Al and Cu targets as described in [24,37]. Briefly, the base pressure of the chamber is consistently below 1.2×10^{-7} mbar prior to any sputtering process. For CuO deposition,

https://doi.org/10.1016/j.combustflame.2019.04.031

To cite it : Combustion and Flame, Volume 205, July 2019, Pages 389-396

the O_2 and Ar flow rates are 100 and 40 SCCM (Square Centimeter Cube per Minute) respectively. The oxygen partial pressure of 5×10^{-3} mbar ensures the stoichiometric ratio of cupric oxide. The Ar partial pressure during Al deposition is maintained at 1×10^{-3} mbar. The substrate temperature is kept at 10 °C for the overall deposition process. To avoid cross contamination in the alternative layers, the chamber is fully pumped to its base pressure after each Al and CuO process.

- TFE from Thin Film Equipment, Italy: a second set of samples were magnetron sputtered from Cu and Al targets (8 by 3 inches sides and ¼ inches thick) using a base pressure of 5×10^{-7} mbar. O_2 and Ar gases flow rates of 16 and 32 SCCM are used respectively for cupric oxide deposition with a partial pressure of 10^{-2} mbar. The Ar partial pressure during Al deposition is maintained at 5×10^{-3} mbar. The Al and Cu targets are localized in the same chamber and the sample stage moves from one target to the other at a speed of 244 $cm.min^{-1}$ and 320 $cm.min^{-1}$ respectively for the deposition of CuO and Al. The sample is cooled at ambient temperature for 600 s at the end of the deposition process.

For each sample, the nanolaminate is characterized by : the equipment used for its growth (TFE or UNIVEX), the bilayer thickness (ω) and the Al to CuO ratio (ς*:1*). Note that in a 1:1 Al/CuO bilayer (ς*=1)*, the aluminum thickness is half the CuO thickness whereas in ς:1 Al/CuO, the Al thickness is $\frac{\varsigma}{2}$ of the CuO thickness, corresponding to a non-stoichiometric situation. 1:1 Al/CuO bilayer (ς*=1)* is a stoichiometric stack.

X-ray diffraction (XRD, Bruker D8 Discover system with a Cu kα radiation source) scans were performed on all samples after deposition. The diffraction peaks in supplementary file **Figure S2** clearly shows the clear polycrystalline nature of cupric oxide, the CuO structure, identified

https://doi.org/10.1016/j.combustflame.2019.04.031

To cite it : Combustion and Flame, Volume 205, July 2019, Pages 389-396

by the JCPDS database (00-048-1548) to be in a preferential orientation along the (-111) plane, for both processes. From a morphological standpoint, the TFE process exhibits slightly denser CuO film, at 6.3 ± 0.2 g.cm^{-3}, compared to TFE, with a density of 5.6 ± 0.2 g.cm^{-3}. In addition, the average CuO grain size are estimated to be much larger for UNIVEX samples : 28.6 ± 10 nm versus 15 ± 4 nm for TFE CuO films. As for the aluminum layers, both UNIVEX and TFE processes show comparable polycrystalline structures with inhomogeneous grains at the sub-micron scale.

It is to be noted that some intermixing is expected between the alternating layers. Abdallah *et al.* found that there is some 4 - 15 nm of intermixing between Al and CuO using the UNIVEX process [13]. We characterized the layers produced by TFE and found that there is some 4-8 nm of intermixing between Al and CuO. As the thinest bilayer produced for this study is 150 nm, the volume fraction of the intermixed regions represents less than 10%, and, therefore, the intermixing is expected to have limited impact on the reaction temperatures and flame velocities.

2.3. Temperature measurements

A multi-wave pyrometry method was used to calculate the temperature of gas and condensed phases produced by the combustion event. The method is similar to that first reported by Ng and Fralick [24]. From Planck's law, the emitted radiation intensity $L(T,\lambda)$ of a diffuse surface in thermal equilibrium, with a given emissivity $\varepsilon(T,\lambda)$ is expressed by Eq. 1 as a function of the temperature (T) and wavelength (λ), where h is the Planck's constant, c_0 is the speed of light in vacuum and k_B is the Boltzmann constant.

$$L(T,\lambda) = \varepsilon(T,\lambda)\frac{C_1}{\lambda^5\left[\exp\left(C_2/\lambda T\right)-1\right]};\ C_1 = 2\pi h c_0^2\ ;\ C_2 = \frac{hc_0}{k_B} \quad (1)$$

https://doi.org/10.1016/j.combustflame.2019.04.031

To cite it : Combustion and Flame, Volume 205, July 2019, Pages 389-396

The knowledge of the correct functional wavelength and temperature dependence of emissivity is crucial for accurate temperature measurement and bad assumptions can lead to great uncertainties in the temperature of 100s to 1000s. The spectral emissivity of copper, copper oxides at elevated temperature (thermite combustion temperature) are still unknown. However, considering aluminum oxide particles clouds, common assumptions of the functional wavelength dependence of emissivity ranges from grey bodies to $1/\lambda^n$ (ranging from 1-2). A work published by Lynch *et al.* [25] showed experimentally that the aluminum oxide particles clouds emissivity is also highly function of temperature. Interestingly, a spectral emissivity dependence in $1/\lambda$ and $1/\lambda^2$ is appropriate for low-temperature measurements (around alumina melting). However at temperature near 3000 K a greybody assumption (independent of the wavelength) is seemingly appropriate whereas above 3500 K a λ dependence is more appropriate. For this study, considering the combustion temperature between 3000 – 3500 K, we assume that emissivity is independent of the wavelength.

Therefore, the Planck's distribution can be written as shown in Eq. 2.

$$ln\left[\frac{C_1}{\lambda^5 L}\right] = {C_2}/{\lambda T} + ln\left[1 - \exp\left({-C_2}/{\lambda T}\right)\right] - \ln \varepsilon \qquad (2)$$

Plotting either the quantity $\frac{ln\left[\frac{C_1}{\lambda^5 L}\right]}{{C_2}/{\lambda}} - \frac{ln\left[1-\exp\left({-C_2}/{\lambda T}\right)\right]}{{C_2}/{\lambda}}$ or $\frac{ln\left[\frac{C_1}{\lambda^5 L}\right]}{{C_2}/{\lambda}}$ as a function of λ is a straight line with a slope of $\frac{-\ln \varepsilon}{C_2}$. The spectral range of 400 – 800 nm was used for this analysis as it features the best detector efficiency.

3. Results and discussions

3.1. Combustion in Air

https://doi.org/10.1016/j.combustflame.2019.04.031
To cite it : Combustion and Flame, Volume 205, July 2019, Pages 389-396

In **Figure 3**, high speed camera results are presented for all samples : TFE versus UNIVEX nanolaminates with varying stoichiometric ratios and bilayer thicknesses. Due to aperture adjustments that are necessary to obtain good images with sufficient contrast, it is not possible to deduce the flame intensity from the relative brightness between samples. Rather, below each image, the notation *vw*, *w*, *m* (very weak, weak, medium respectively) gives the indication of the flame intensity derived from emission spectroscopy data. For all samples, the flame color is bright white close to the propagation front and propagates in a single direction. From the inhomogeneities within the flame, we can deduce that small particles are ejected from the propagation front and burn in the air. There is also a strong and extended haze associated with the reaction meaning that gaseous species are being created during Al/CuO reaction. Snapshots also show an inclination of the flame in samples featuring the highest combustion rates (9 and 19.9 $m.s^{-1}$). Average flame velocities for each samples are given in **Figure 4**.

At a constant stoichiometric ratio, we observed that the average flame velocity decreases when bilayer thickness increases, which is a well-known trend previously described in the literature. We note that Al-rich compositions (i.e. 2:1 Al/CuO) burn the fastest, in concurrence with previously published results [26].

The TFE deposition technique produces much more reactive nanolaminates, exhibiting systematically higher velocities compared to UNIVEX samples (between 1.5 to 2 times). The fastest flame velocity, 19.9 $m.s^{-1}$, is obtained for the TFE Al-rich sample with a bilayer thickness of 200 nm. The same multilayer grown on UNIVEX burns at only 9 $m.s^{-1}$, emphasizing the crucial role of synthesis conditions and mechanical properties of each layer on combustion performances.

https://doi.org/10.1016/j.combustflame.2019.04.031
To cite it : Combustion and Flame, Volume 205, July 2019, Pages 389-396

Next the emission spectra captured during the flame propagation in air are plotted in **Figure 5** for each sample. It has to be noted here that the emission spectra taken in this study are not spatially resolved; therefore, it represents a convolution of the spectra emitted by the flame during the combustion event without distinguishing the accurate position (near surface or in the plume). All spectra indicate major and reproducible peaks that allow assignations. Although we cannot isolate which specific species is produced during the reaction, the spectra point to the fact that copper vapor, from Cu and CuO decomposition, is produced : Cu II 608, 627, 655 nm), Cu_2O (Cu III 596 nm) and Cu (Cu I 578 nm). In addition to CuO peaks, strong lines appearing at 473, 485, 513 nm are detected within all samples and are attributed to AlO vapor [27]. Based on this observation, there is clear aluminum combustion taking place in the air. In addition, the numerous Cu II peaks would indicate that gaseous products are produced during the reaction; these products may cause some CuO emission after reacting with the oxygen in the air or with the decomposition products from the unreacted nanothermite. Finally, emission of atomic Al (397 nm) is detected exclusively in the 2:1 Al/CuO samples, which may validate the claim that the nanothermite disintegrates before the redox reaction is completed.

The differences in the peaks' intensities observed for the different Al/CuO samples, can be explained by the quantity of the Al pieces ejected. Thick bilayers (ω > 200 nm) eject more and coarser Al pieces that burns into the air. Microscopy images of reaction debris (**Figure 6**) that have been collected after the combustion show that the nanolaminates produced two types of residues: micron-sized spherical particles of alumina (2–7 µm in diameter) mixed with bigger (10 – 50 µm in size) random shaped aggregates made of two components : alumina and copper (See supplementary information file S3 for chemical mapping). In addition, it is clearly observed in SEM photographs that the quantity and size of residues is much important for thick

https://doi.org/10.1016/j.combustflame.2019.04.031

To cite it : Combustion and Flame, Volume 205, July 2019, Pages 389-396

bilayer than for thin one. 2:1 Al/CuO samples with ω = 400 nm produce ~ 280 residues / mm² featuring size ranging from 2 – 50 µm whereas 2:1 Al/CuO samples with ω = 200 nm produce ~15 residues /mm² with roughly same dispersion in size (2 - 30 µm).

Considering Al-rich samples, the correlation between the emitted species in the gas and condensed phase and flame velocity is not straightforward, but a few conclusions are possible. The presence of AlO in the gas phase is detected in samples featuring the fastest flame velocities, contrary to the presence of Cu II peaks, which are in higher quantities for samples featuring slower flame velocities. This could indicate less-completed redox reactions.

For all samples, the gas and condensed phase temperature, commonly referred to as the flame temperature, is calculated from the continuous part of the flame spectrum using Eq. 2 and reported in **Table 1** for each sample configuration. For the fuel-rich samples, the temperature is well above 3000 K, consistent with vapor phase Al combustion. The hottest flame is found to occur in samples with the thickest bilayers. For stoichiometric samples, the flame temperature is ~2800 K. Independent of the multilayer composition and bilayer thickness, the calculated flame temperatures are (i) above the Al vaporization point (2740 K) and the Al_2O_3 melting point (2345 K); (ii) in particular conditions (fuel-rich and thick bilayers grown in TFE), it could be above the Al_2O_3 vaporization point (3248 [28] - 4000 K [29]). These findings are in good agreement with several studies that measured temperatures around 3350 – 3800 K for both Al/oxide [22] and Al combustion [30, 31]. Nevertheless, in [22] it has to be noted that these values (3350 – 3800 K) are overestimated as the authors preheated the systems over 1000 K.

3.2. Combustion in N_2

Focusing exclusively on the TFE samples that show the highest burning rates and flame temperatures, the same experiments were repeated in N_2 atmosphere. Results in terms of flame

DRAFT

https://doi.org/10.1016/j.combustflame.2019.04.031
To cite it : Combustion and Flame, Volume 205, July 2019, Pages 389-396

velocity, flame temperature, as well as the emission spectra were compared with those obtained in air.

For all nanolaminates, the reaction propagates faster in air than in N_2 (**Figure 7**), indicating that environmental oxygen contributes in the Al oxidation. Under N_2, the reaction front burns between 5 and 40 % slower than under air. The same tendency is observed for the flame temperature (see **Table 1**) : it slightly decreases when combustion occurs under N_2 instead of air while remaining above the aluminum vaporization temperature.

Figure 8 compares the emission spectra acquired during the combustion of the TFE grown Al/CuO nanolaminates in air versus in an N_2 atmosphere. In all cases, the AlO signature is highly reduced, indicating that the amount of AlO in the gas phase is reduced. On the contrary, the peaks at 655 nm (assigned to Cu II) keep their intensity in both conditions, implying that the CuO is highly present in the gas phase under N_2, possibly due to an uncompleted reaction. Note that in the fuel-rich configuration (2:1 Al/CuO stacks), the aluminum peak at ~397 is consistently visible whether in air or an N_2 environment. The results of the experiments under N_2 prove that, while oxygen from the air contributes to the Al burning in the gas phase, some oxygen in the reaction is provided by the CuO ejected from the substrate. This could indicate that the flame is composed of droplets of CuO_x and Al or Al:CuO melted aggregates. This is in coherence with the collected combustion debris composed of small alumina particles and big alumina:Cu aggregates (See supplementary File S3).

3.3. Combustion scenario

DRAFT

https://doi.org/10.1016/j.combustflame.2019.04.031
To cite it : Combustion and Flame, Volume 205, July 2019, Pages 389-396

The flame velocity and emission spectra analyses completed in this work have allowed the construction of the following fundamental description of the self-propagating reaction scenario in Al/CuO nanolaminates (depicted in **Figure 9**).

Upon heating (**Figure 9a**), the redox reaction begins between the Al and CuO reactant layers in the bulk material. In the reaction zone, the temperature quickly increases and produces the disintegration of the nanolaminate before the entire Al reservoir has reacted (**Figure 9b).** This explains why the observed flame temperature is above the Al vaporization point and, even, in some particular conditions, above the Al_2O_3 vaporization point. The disintegration of the multilayers prior to reaction completeness can be explained by two factors: (i) the vaporization of reactants (such as Al or CuO_x) within the first multilayers causing its disintegration before the heat propagates throughout the entire thickness. (ii) stress-induced mechanical rupture upon heating prior to the completion of the reaction. When the multilayer structure breaks apart, it disperses in the ambient unreacted, melted Al and CuO. Both continue to react, now with the additional possibility for unreacted Al to burn with environmental oxidizers such as those found in air (**Figure 9c**). The temperature at which the multilayer film tears off the substrate is very difficult to estimate. Not only does it depend on the reactants' nature providing well-tabulated vaporization temperatures, it is also highly dependent on the bilayer residual-stress, which is highly controlled by the deposition conditions. A high-stressed thin bilayer (> 100 MPa) may tear off the substrate at very low temperatures, likely well below CuO or Al boiling points, whereas a low-stressed thin bilayer (< 20 MPa) may sustain higher temperatures prior to its disintegration.

This self-propagating combustion scenario is a possible explanation of *the high difference in the flame temperature and velocity* measured for similar multilayers grown from two different

https://doi.org/10.1016/j.combustflame.2019.04.031
To cite it : Combustion and Flame, Volume 205, July 2019, Pages 389-396

processes. The stress of the UNIVEX grown CuO/Al and Al/CuO bilayer is 42 MPa and 28 MPa, respectively, against 12 MPa and 8 MPa for the bilayers grown using TFE equipment. We conjecture that the UNIVEX multilayers tear off the substrate at low temperature, leaving behind coarse unreacted fragments of Al. Melted pieces of Al and CuO may then continue reacting in the environment. TFE grown multilayers tear off the substrate at high temperature, after the CuO is vaporized. Note also that TFE produces a denser CuO, i.e., containing less than 10 % of O in addition to UNIVEX grown CuO. This allows, at equivalent bilayer thickness, to increase the completion of Al reaction, directly impacting the reaction temperature. This may explain the greater production of light, ejected particles, and gaseous species observed for TFE samples

4. Conclusion

This experimental study provides novel insights into the self-propagating reaction in Al/CuO nanolaminates through the combination of high-speed imaging and optical spectroscopy measurements. The flame velocity and emission spectra were analyzed, leading to the following conclusions:

- The combustion regime, as provided by the flame characterization indicates a high temperature regime (> 3000 K for TFE) around the vaporization temperature of alumina, with clear evidence of both AlO signatures. As videos showed particle ejection and haze, we deduced that the redox reaction starts in the nanolaminate, which then rapidly tears off the substrate to continue burning in condensed and gas phase in the environment.

- The flame temperature increases with stoichiometry but is independent of the bilayer thickness. Al-rich nanolaminates may eject coarser Al pieces into the environment, thereby producing hotter burn temperatures even in a controlled atmosphere (N_2). This suggests that most of the exothermic process takes place either in the condensed phase

https://doi.org/10.1016/j.combustflame.2019.04.031

To cite it : Combustion and Flame, Volume 205, July 2019, Pages 389-396

or in the gas phase in the immediate vicinity of the reaction zone, close to the surface of the nanolaminate.

- The film's residual-stress, which depends on the deposition conditions, influence the propagation and flame characteristics.

These results confirm the complexity of the Al/CuO self-propagating reaction mechanisms, which include multi-phase and multi-species dynamics (gaseous, condensed and probably heterogeneous) occurring at different lengths in mostly non-equilibrium conditions. To advance our current understanding of these reactions, it will require further measurements with advanced *in-situ* instrumentation including time and spatially-resolved spectroscopy, imaging and diffraction techniques to better analyze the combustion event.

Acknowledgements

We thank Severine Vivies for its collaboration in producing a large numbers of multilayer samples. We thank the European Commission and Region Occitanie for their FEDER support (THERMIE grant) having partially funded the sputter-deposition equipement. We also thank the European Research Council as well as the university Fédérale de Toulouse for its financial support through the PyroSafe project (grant number 832889) and "chaire d'attractivité" MUSE, respectively.

Bibliography

[1] A. Nicollet, L. Salvagnac, V. Baijot, A. Estève, C. Rossi, Fast circuit breaker based on integration of Al/CuO nanothermites, Sensor Actuat a-Phys 273 (2018).
[2] L. Glavier, A. Nicollet, F. Jouot, B. Martin, J. Barberon, L. Renaud, C. Rossi, Nanothermite/RDX-Based Miniature Device for Impact Ignition of High Explosives, Propell Explos Pyrot 42 (2017) 307-316.
[3] G. Taton, D. Lagrange, V. Conedera, L. Renaud, C. Rossi, Micro-chip initiator realized by integrating Al/CuO multilayer nanothermite on polymeric membrane, J Micromech Microeng 23 (2013).

DRAFT

https://doi.org/10.1016/j.combustflame.2019.04.031

To cite it : Combustion and Flame, Volume 205, July 2019, Pages 389-396

[4] L. Glavier, G. Taton, J.M. Ducere, V. Baijot, S. Pinon, T. Calais, A. Esteve, M.D. Rouhani, C. Rossi, Nanoenergetics as pressure generator for nontoxic impact primers: Comparison of Al/Bi2O3, Al/CuO, Al/MoO3 nanothermites and Al/PTFE, Combust Flame 162 (2015) 1813-1820.
[5] A.H. Kinsey, K. Slusarski, S. Sosa, T.P. Weihs, Gas Suppression via Copper Interlayers in Magnetron Sputtered Al-Cu2O Multilayers, Acs Appl Mater Inter 9 (2017) 22026-22036.
[6] J.L. Yi, Y.P. Zhang, X.X. Wang, C.L. Dong, H.C. Hu, Characterization of Al/Ti Nano Multilayer as a Jointing Material at the Interface between Cu and Al2O3, Mater Trans 57 (2016) 1494-1497.
[7] A. Duckham, Applying localized heat for brazing and soldering, Weld J 85 (2006) 44-46.
[8] X. Zhou, R.Q. Shen, Y.H. Ye, P. Zhu, Y. Hu, L.Z. Wu, Influence of Al/CuO reactive multilayer films additives on exploding foil initiator, J Appl Phys 110 (2011).
[9] P. Zhu, R.Q. Shen, Y.H. Ye, S. Fu, D.L. Li, Characterization of Al/CuO nanoenergetic multilayer films integrated with semiconductor bridge for initiator applications, J Appl Phys 113 (2013).
[10] P. Zhu, R.Q. Shen, Y.H. Ye, X. Zhou, Y. Hu, L.Z. Wu, Energetic Igniters Based on Al/CuO/B/Ti Reactive Multilayer Films, Theory and Practice of Energetic Materials (Vol Ix), Proceedings of the 2011 International Autumn Seminar on Propellants, Explosives and Pyrotechnics, (2011) 756-760.
[11] A. Nicollet, G. Lahiner, A. Belisario, S. Souleille, M. Djafari-Rouhani, A. Esteve, C. Rossi, Investigation of Al/CuO multilayered thermite ignition, J Appl Phys 121 (2017).
[12] M. Bahrami, G. Taton, V. Conedera, L. Salvagnac, C. Tenailleau, P. Alphonse, C. Rossi, Magnetron Sputtered Al-CuO Nanolaminates: Effect of Stoichiometry and Layers Thickness on Energy Release and Burning Rate, Propell Explos Pyrot 39 (2014) 365-373.
[13] I. Abdallah, J. Zapata, G. Lahiner, B. Warot-Fonrose, J. Cure, Y. Chabal, A. Esteve, C. Rossi, Structure and Chemical Characterization at the Atomic Level of Reactions in Al/CuO Multilayers, ACS Applied Energy Materials 1 (2018) 17-62.
[14] G.C. Egan, E.J. Mily, J.P. Maria, M.R. Zachariah, Probing the Reaction Dynamics of Thermite Nanolaminates, J Phys Chem C 119 (2015) 20401-20408.
[15] K.J. Blobaum, A.J. Wagner, J.M. Plitzko, D. Van Heerden, D.H. Fairbrother, T.P. Weihs, Investigating the reaction path and growth kinetics in CuOx/Al multilayer foils, J Appl Phys 94 (2003) 2923-2929.
[16] E.J. Mily, A. Oni, J.M. LeBeau, Y. Liu, H.J. Brown-Shaklee, J.F. Ihlefeld, J.P. Maria, The role of terminal oxide structure and properties in nanothermite reactions, Thin Solid Films 562 (2014) 405-410.
[17] G. Lahiner, A. Nicollet, J. Zapata, L. Marín, N. Richard, M. Djafari-Rouhani, C. Rossi, A. Estève, A diffusion–reaction scheme for modeling ignition and self-propagating reactions in Al/CuO multilayered thin films J Appl Phys 122 (2017).
[18] M. Petrantoni, C. Rossi, L. Salvagnac, V. Conedera, A. Esteve, C. Tenailleau, P. Alphonse, Y.J. Chabal, Multilayered Al/CuO thermite formation by reactive magnetron sputtering: Nano versus micro, J Appl Phys 108 (2010).
[19] J.B. DeLisio, F. Yi, D.A. LaVan, M.R. Zachariah, High Heating Rate Reaction Dynamics of Al/CuO Nanolaminates by Nanocalorimetry-Coupled Time-of-Flight Mass Spectrometry, J Phys Chem C 121 (2017) 2771-2777.
[20] C. Rossi, Engineering of Al/CuO reactive multilayer thin films for tunable initiation and actuation, Propellants, Explosives, Pyrotechnics 44 (2019) 94-108.
[21] K.T. Sullivan, O. Cervantes, J.M. Densmore, J.D. Kuntz, A.E. Gash, J.D. Molitoris, Quantifying Dynamic Processes in Reactive Materials: An Extended Burn Tube Test, Propell Explos Pyrot 40 (2015) 394-401.
[22] T. Bazyn, N. Glumac, H. Krier, T.S. Ward, M. Schoenitz, E.L. Dreizin, Reflected shock ignition and combustion of aluminum and nanocomposite thermite powders, Combust Sci Technol 179 (2007) 457-476.
[23] H.Y. Feng, L. Zhang, S.G. Zhu, R. Wu, Y. Li, R.Q. Shen, Research on the Temperature and Its Duration of Semiconductor-Bridge Plasma, Ieee T Plasma Sci 37 (2009) 1830-1835.

https://doi.org/10.1016/j.combustflame.2019.04.031

To cite it : Combustion and Flame, Volume 205, July 2019, Pages 389-396

[24] D. Ng, G. Fralick, Use of a multiwavelength pyrometer in several elevated temperature aerospace applications, Rev Sci Instrum 72 (2001) 1522-1530.
[25] P. Lynch, H. Krier, N. Glumac, Emissivity of Aluminum-Oxide Particle Clouds: Application to Pyrometry of Explosive Fireballs, J Thermophys Heat Tr 24 (2010) 301-308.
[26] J.J. Granier, M.L. Pantoya, Laser ignition of nanocomposite thermites, Combust Flame 138 (2004) 373-383.
[27] S. Goroshin, J. Mamen, A. Higgins, T. Bazyn, N. Glumac, H. Krier, Emission spectroscopy of flame fronts in aluminum suspensions, P Combust Inst 31 (2007) 2011-2019.
[28] D. Linne, Handbook of Chemistry and Physics, CRC Press, Cleveland, OH, 2007/2008.
[29] M. Chase, NIST-JANAF Thermochemical Tables, 4th ed., American Chemical Society Press, New York, NY, 1998.
[30] P. Lynch, H. Krier, N. Glumac, Micro-alumina particle volatilization temperature measurements in a heterogeneous shock tube, Combust Flame 159 (2012) 793-801.
[31] E.L. Dreizin, Experimental study of stages in aluminum particle combustion in air, Combust Flame 105 (1996) 541-556.

DRAFT

Table 1. Flame temperature (in air and in N_2) derived from the raw continuous spectra as a function of different bilayer thicknesses (ω) and Al:CuO ratios. In parenthesis are the measurements uncertainties.

Al:CuO ratio	*Bilayer Thickness*	*Temperature [K]*

https://doi.org/10.1016/j.combustflame.2019.04.031

To cite it : Combustion and Flame, Volume 205, July 2019, Pages 389-396

	ω [nm]	Air	N_2
1:1	150	2917 (14)	2683 (10)
	300	2959 (16)	2758 (14)
2:1	200	3651 (19)	3235 (9)
	400	3845 (30)	3657 (22)

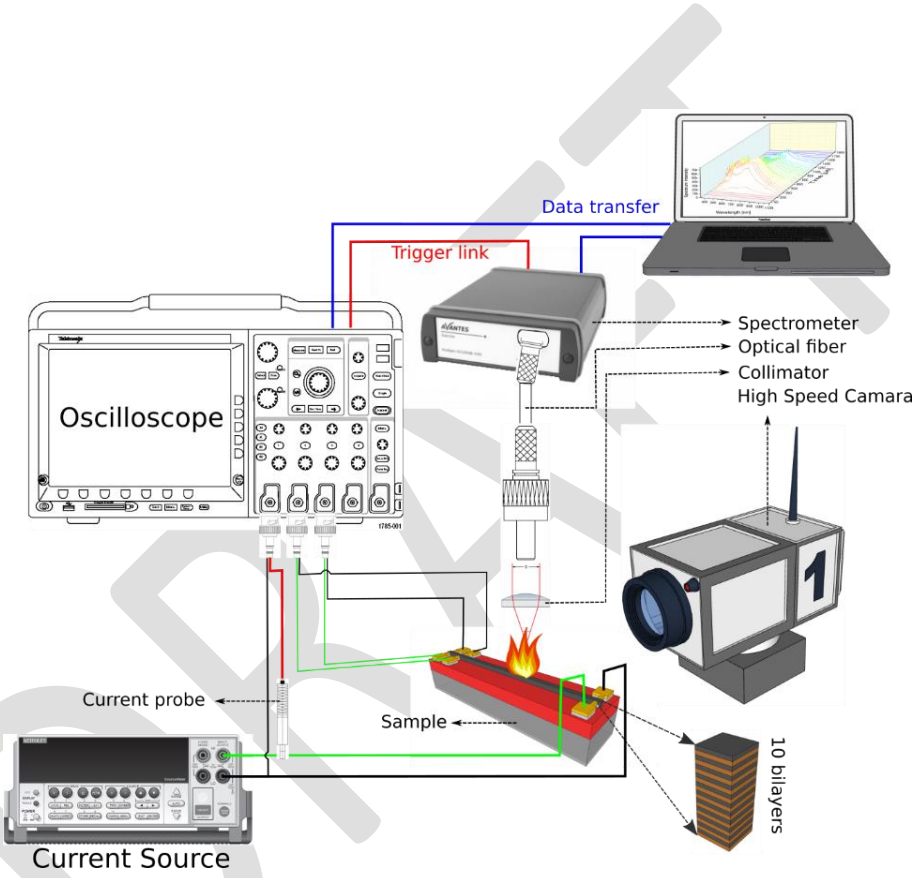

Figure 1. Schematic of the self-propagating reaction front characterization set up used in this study.

https://doi.org/10.1016/j.combustflame.2019.04.031

To cite it : Combustion and Flame, Volume 205, July 2019, Pages 389-396

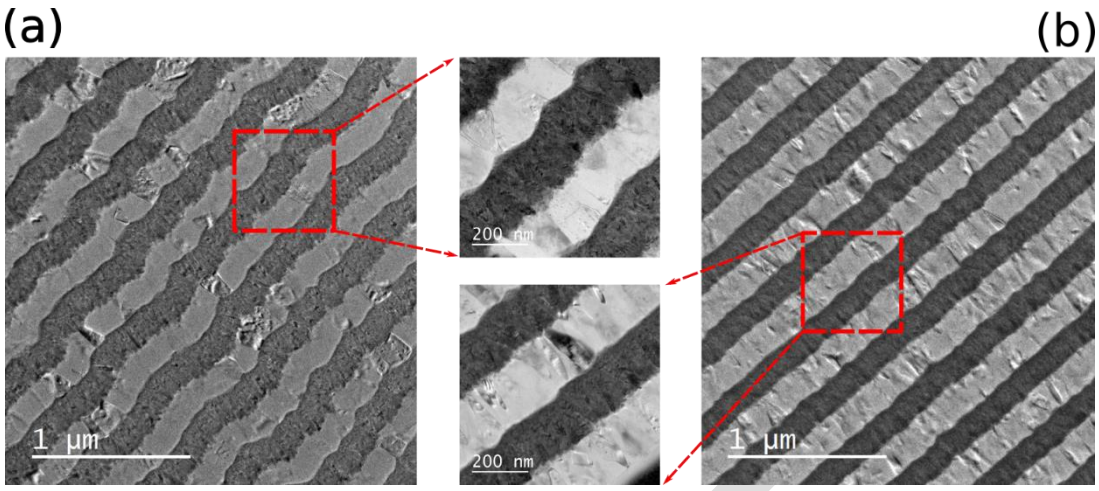

Figure 2. Transmission electron micrographs of the cross section of Al/CuO nanolaminates obtained by reactive DC magnetron sputtering. (a) ten 400 nm thick 2:1 bilayers grown on UNIVEX, (b) ten 400 nm thick 2:1 Al/CuO grown on TFE.

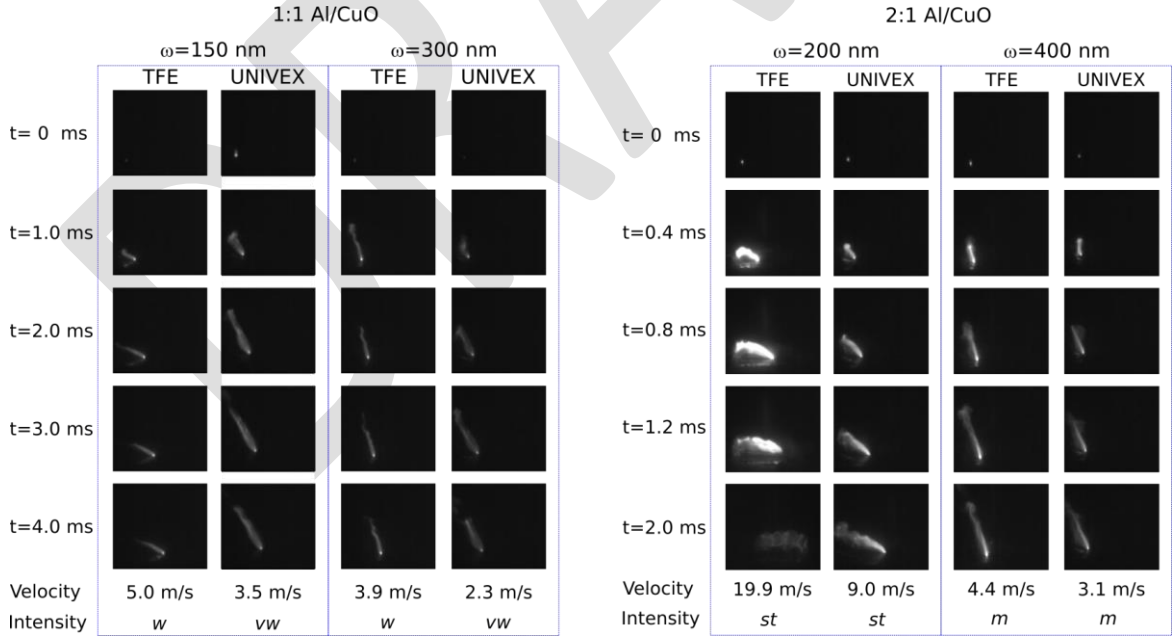

Figure 3. High-speed snapshots of Al/CuO nanolaminates self-propagating combustion in air. The average flame velocities calculated from the images are reported below snapshots.

https://doi.org/10.1016/j.combustflame.2019.04.031

To cite it : Combustion and Flame, Volume 205, July 2019, Pages 389-396

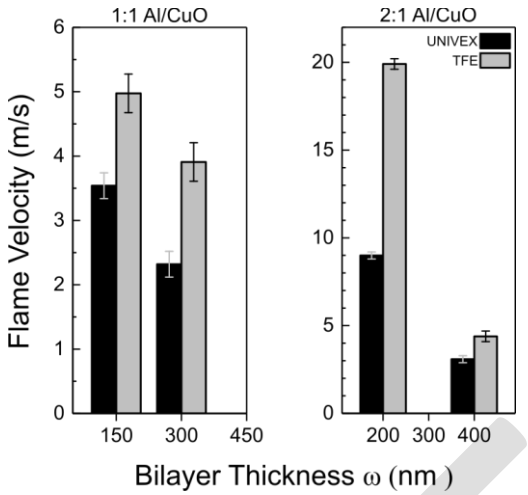

Figure 4. Average flame velocity under air as a function of bilayer thickness (ω) for two Al to CuO ratios : stoichiometric and fuel-rich stacks. Solid and shaded rectangles correspond to samples grown on UNIVEX and TFE, respectively.

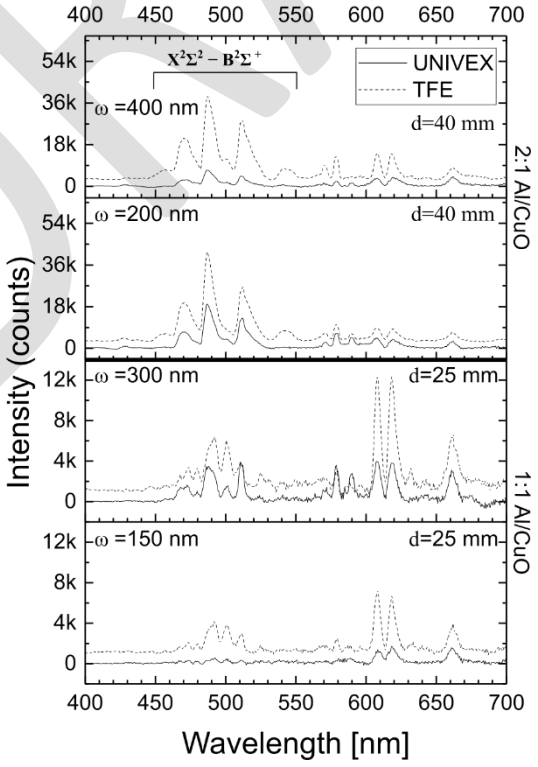

DRAFT

https://doi.org/10.1016/j.combustflame.2019.04.031

To cite it : Combustion and Flame, Volume 205, July 2019, Pages 389-396

Figure 5. Emission spectra of the combustion of Al/CuO nanolaminates under air with different stoichiometric ratios and bilayer thicknesses (ω). In order to have a better visualization, the spectra of the samples burned in air are shifted to slightly higher intensity (from +1K for 1:1 stoichiometry to +3K for 2:1 stoichiometry). d is the distance between the collimator and the sample.

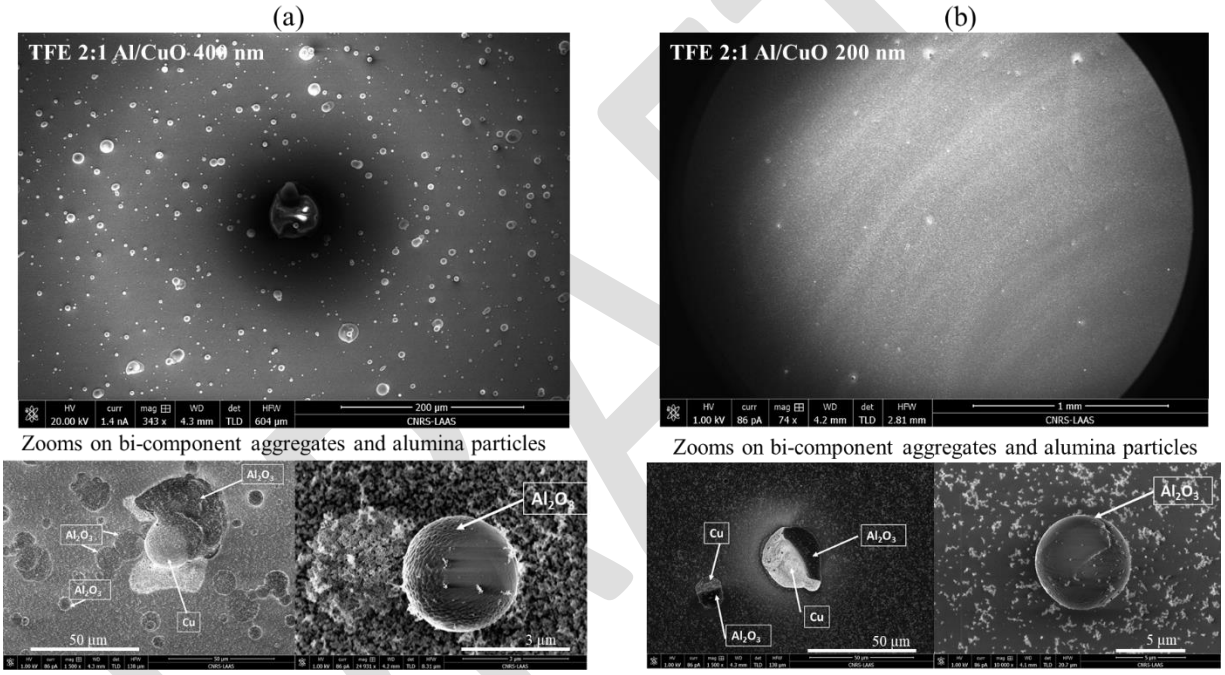

Figure 6. SEM images (Helios 600i instrument) showing products of reaction collected for samples grown on TFE with 2:1 stoichiometry and bilayer thickness of 400 nm (a) and 200 nm (b). The chemical composition was determined using EDS analysis shown in supplementary file Figure S3.

https://doi.org/10.1016/j.combustflame.2019.04.031

To cite it : Combustion and Flame, Volume 205, July 2019, Pages 389-396

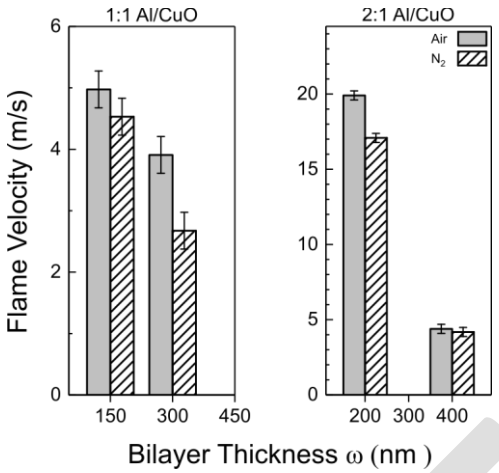

Figure 7. Average flame velocity under air and N_2 environments as a function of bilayer thickness (ω) for two Al to CuO ratios : stoichiometric and fuel-rich stacks. Solid and dotted rectangles correspond to experiments performed in air and N_2 conditions, respectively.

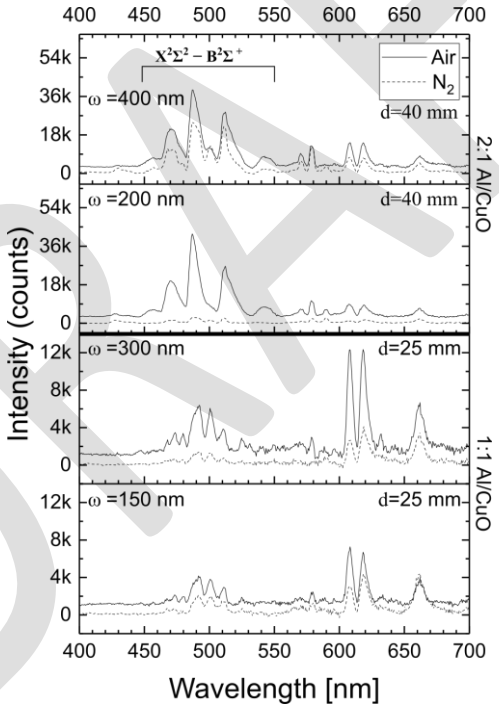

Figure 8. Emission spectra of the combustion of Al/CuO nanolaminates under N_2 and air. All samples were grown on TFE and have different stoichiometric ratios and bilayer thicknesses. In order to better visualize, the spectra of the samples burned in air are shifted to slightly higher intensity (from +1K for 1:1 stoichiometry to +3K for 2:1 stoichiometry). d corresponds to the distance between the collimator and the sample.

DRAFT

https://doi.org/10.1016/j.combustflame.2019.04.031

To cite it : Combustion and Flame, Volume 205, July 2019, Pages 389-396

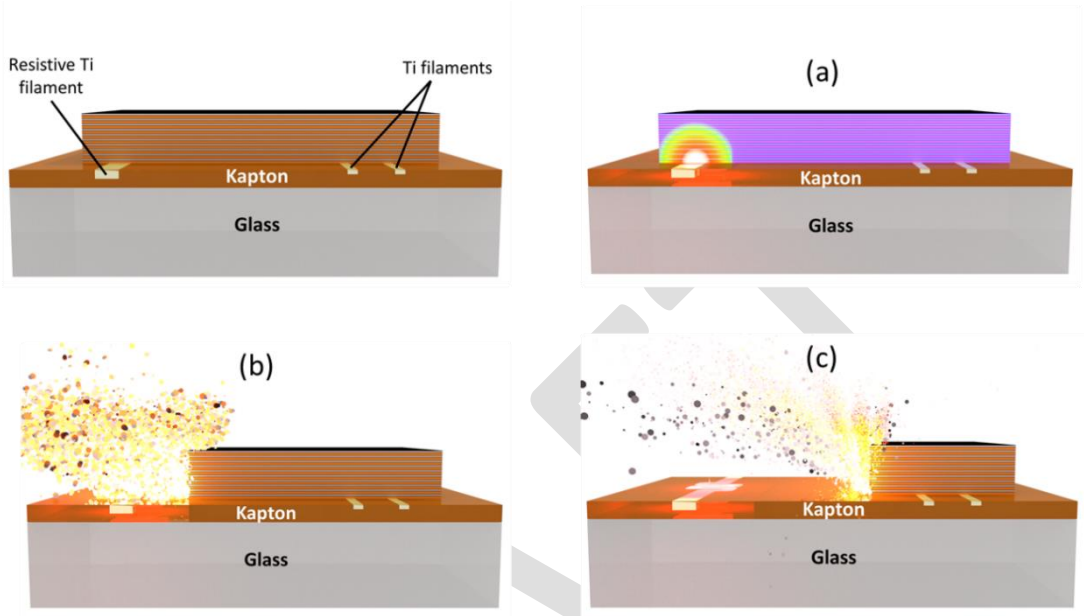

Figure 9. Schematic of the different steps of the self-propagating combustion in Al/CuO nanolaminates.

DRAFT